Immunoreactivity for the GABAA Receptor α1 Subunit, Somatostatin and Connexin36 Distinguishes Axoaxonic, Basket, and Bistratified Interneurons of the Rat Hippocampus

Agnès Baude[1,2], Catherine Bleasdale[1], Yannis Dalezios[1,3,4], Peter Somogyi[1] and Thomas Klausberger[1,5]

[1]MRC Anatomical Neuropharmacology Unit, Department of Pharmacology, Oxford University, Oxford OX1 3TH, UK, [2]CNRS UMR 6150, IFR Jean Roche, Faculty of Medicine Nord, University Aix-Marseille II, France, [3]Department of Basic Sciences, Faculty of Medicine, University of Crete, Heraklion, Greece, [4]Institute of Applied and Computational Mathematics, Foundation of Research and Technology, Hellas, Heraklion, Greece and [5]Center for Brain Research, Medical University Vienna, 1090 Vienna, Austria

Parvalbumin (PV)-expressing interneurons synchronize cortical neurons through γ-aminobutyric acidergic (GABAergic) synapses. Three types of PV-containing interneurons populate stratum pyramidale of the hippocampal CA1 area: basket cells targeting somata and proximal dendrites, axoaxonic cells innervating axon initial segments, and bistratified cells targeting the dendrites of pyramidal cells. We tested whether this axonal specialization is accompanied by a differential expression of molecules involved in neuronal signaling. Immunofluorescence evaluation of interneurons labeled by neurobiotin in vivo shows that axoaxonic cells express significantly less GABAA receptor α1 subunit in the plasma membrane than basket and bistratified cells. Electron microscopic immunogold labeling reveals that this subunit contributes heavily to extrasynaptic receptors providing a substrate for tonic inhibition. Results from additional immunofluorescence experiments were consistent with the finding that only bistratified cells express the neuropeptide somatostatin. From the molecular profiles, we estimate that basket, bistratified, and axoaxonic cells represent about 60%, 25%, and 15%, respectively, of PV-containing cells in CA1 stratum pyramidale. In addition, all 3 interneuron classes form connexin36-immunopositive dendrodendritic gap junctions. The differential expression of signaling molecules and the relative frequency of cells reflect the specialized temporal contribution of the 3 types of PV-positive interneurons to GABA release in the network.

Keywords: extrasynaptic receptor, firing pattern, gap junction, immunofluorescence, parvalbumin, tonic inhibition

Introduction

Parvalbumin (PV)-expressing interneurons are involved in synchronizing cortical pyramidal cells at various frequencies through γ-aminobutyric acid (GABAA) receptor-mediated synaptic action, provide shunting inhibition, influence the time window for synaptic plasticity, and may even have an excitatory postsynaptic effect (Kawaguchi and Kubota 1997; Tamas et al. 2000; Pouille and Scanziani 2001; Bartos et al. 2002; Pawelzik et al. 2002; Klausberger et al. 2003, 2004; Markram et al. 2004; Szabadics et al. 2006; Vida et al. 2006). The PV-expressing interneurons are not a homogeneous population, and in the pyramidal cell layer of the CA1 area of rat hippocampus, 3 classes of PV-expressing interneurons are distinguished on the basis of their axonal target specificity: axoaxonic cells innervate axon initial segments, basket cells innervate cell bodies and proximal dendrites, and bistratified cells innervate dendrites of pyramidal cells in strata radiatum and oriens (Freund and Buzsaki 1996; Somogyi and Klausberger 2005). An additional GABAergic neuron that expresses PV in the rat (Klausberger et al. 2003), the oriens-lacunosum moleculare (O-LM) cell, is mainly located in stratum oriens and probably occurs rarely, if at all, in the pyramidal cell layer (but see Oliva et al. 2000 in the mouse). During in vivo network oscillations, the different classes of PV-expressing interneurons have distinct firing times and frequencies and therefore provide differential GABAergic input to distinct domains of the pyramidal cells (Klausberger et al. 2003, 2004). In other interneuron classes, specialization in synaptic connections is associated with a specific expression of different receptors, Ca^{2+}-binding proteins, or neuropeptides (Freund and Buzsaki 1996; Somogyi and Klausberger 2005; Sugino et al. 2006). However, for PV-expressing axoaxonic, basket, and bistratified cells, no discriminating molecular pattern has been identified directly so far. Following previous sporadic observations in our molecular analysis of recorded neurons, in the present study, we tested directly a potential differential expression of the α1 subunit of GABAA receptors (α1-GABAARs), the neuropeptide somatostatin (SOM), and the gap junction–forming protein connexin36 (Cx36) in the 3 cell classes.

The α1-GABAAR is expressed by principal cells and interneurons in the hippocampus (Wisden et al. 1992), and immunoreactivity for α1-GABAAR is present in all layers of the CA1 area (Gao and Fritschy 1994; Pirker et al. 2000). Many PV-containing interneurons express α1-GABAAR, and a strong immunoreactivity of cell bodies and dendrites stands out from the relatively weak and diffuse immunolabeling of the neuropil (Gao and Fritschy 1994; Mohler et al. 1995; Nusser, Roberts, Baude, Richards, Sieghart, et al. 1995). It is possible that this strong α1-GABAAR immunoreactivity represents extrasynaptic GABAA receptors contributing to the strong tonic inhibition of hippocampal interneurons (Semyanov et al. 2003), as in the dentate gyrus (Nusser, Roberts, Baude, Richards, Sieghart, et al. 1995).

In the CA1 area, the neuropeptide SOM is expressed in O-LM (Baude et al. 1993; Losonczy et al. 2002; Klausberger et al. 2003; Ferraguti et al. 2004), hippocamposeptal (Gulyas et al. 2003), and PV-expressing bistratified cells (Klausberger et al. 2004). The absence of SOM in basket and axoaxonic cells providing perisomatic innervation has been suggested but tested so far only on a small sample of in vitro labeled basket cells in the mouse (Losonczy et al. 2002). It has also been suggested that some cells innervating the axon initial segment in the neocortex express SOM (Gonchar et al. 2002).

Cortical PV-expressing interneurons express Cx36 and are interconnected through gap junctions as established by electron microscopy (Fukuda and Kosaka 2003; Fukuda et al. 2006). Electrophysiological recordings have demonstrated electrical coupling (Galarreta and Hestrin 1999; Gibson et al. 1999; Meyer et al. 2002) and gap junctions (Tamas et al. 2000) between

PV-expressing cells and also between other cortical interneuron classes (Gibson et al. 1999; Szabadics et al. 2001; Galarreta et al. 2004; Price et al. 2005; Zsiros and Maccaferri 2005). Several molecular species of connexins, proteins constitutive of gap junctions, have been described in the brain (Bruzzone et al. 2003; Condorelli et al. 2003; Connors and Long 2004). Amongst them, Cx36 is very likely to be expressed in hippocampal interneurons (Venance et al. 2000; Weickert et al. 2005). To test if all 3 classes of PV-expressing interneurons in stratum pyramidale of the CA1 area form gap junctions, we performed immunofluorescent labeling with antibodies to Cx36 on identified interneurons.

Materials and Methods

All procedures involving experimental animals were carried out under a Home Office project license in accordance with the UK Animals (Scientific Procedures) Act 1986 and associated procedures. All efforts were made to minimize stress to the animals and the number of animals used.

In Vivo Recordings, Labeling, and Physiological Data Analysis

Extracellular recording followed by juxtacellular labeling was performed as previously described (Klausberger et al. 2003, 2004). Briefly, male Sprague–Dawley rats (250–350 g) were anesthetized with urethane (1.25 g per kg of body weight) plus supplemental doses of ketamine and xylazine (20 and 2 mg/kg, respectively) as needed. Neuronal activity in the hippocampus was recorded extracellularly with a glass electrode (15–25 MΩ) filled with 1.5% neurobiotin in 0.5 M NaCl, and the local field potential (LFP) was recorded with the same electrode or a nearby second electrode in the hippocampal CA1 pyramidal cell layer. Single unit activity (sampling rate 20 kHz) and LFP (sampling rate 1 kHz) were filtered online between 0.8–5 kHz and 0.3–300 Hz, respectively. Action potentials were recorded without touching the cell with the electrode, to avoid the risk of altering the firing pattern. After recording the firing patterns of the cell during different network oscillations, the electrode was advanced toward the cell and the cell was labeled juxtacellularly with neurobiotin by applying positive current steps (Pinault 1996). The shape and amplitude of spikes were monitored during recording, advancing the electrode, and labeling the cell to ensure that recorded spikes originated from a single neuron only and that the recorded cell was labeled. The rats were perfused with fixative 4 h after labeling; the fixative was composed of 4% paraformaldehyde, ~0.2% picric acid, and 0.05% glutaraldehyde made up in 0.1 M sodium phosphate buffer (PB, pH 7.2–7.4).

Immunocytochemistry

After in vivo labeling and perfusion, brains were removed, extensively rinsed in PB, and serially sectioned in the coronal plane on a vibratome at 60, 65, or 70 μm thickness. Sections were kept in PB containing 0.05% sodium azide waiting for further immunofluorescence or peroxidase reactions. Five additional adult Sprague–Dawley rats, used for immunofluorescence and preembedding immunogold reactions, were deeply anesthetized with sagatal (pentobarbitone sodium; 100 mg/kg, intraperitoneally [i.p.]) or ketamine and xylazine (100 and 10 mg/kg, respectively, i.p.) and transcardially perfused with saline, followed by the fixative composed as above for 15 min.

Immunofluorescence experiments were carried out according to previously published procedures (Klausberger et al. 2003, 2004; Somogyi et al. 2004). Briefly, free-floating sections were blocked by incubation in 20% normal horse serum for 1 h and then incubated for approximately 48 h (4 °C) in streptavidine coupled to Alexa 488 (Al488; 1:1000, Jackson Immunoresearch Laboratories Inc., West Grove, PA) or to AMCA ([6-((7-amino-4-methylcoumarin-3-acetyl)amino)]; 1:1000, Vector Laboratories, Burlingame, CA) to detect neurobiotin, when necessary. A mixture of primary antibodies containing the antibody directed to the N-terminal part of α1-GABA$_A$R and antibodies to PV, Cx36, or SOM (see Table 1 for complete listing and dilutions), made up in 0.9% NaCl buffered with 50 mM Tris (TBS, pH 7.4) and also containing 1% normal horse serum and 0.3% Triton X-100, was used. After extensive washes in TBS, sections were incubated overnight (4 °C) with a mixture of appropriate secondary antibodies (1:500) coupled to various fluorophores (Al488, Cy3™, Cy5™) purchased from commercial suppliers (Jackson Immunoresearch Laboratories, Inc.; Molecular Probes Invitrogen Corp., Carlsbad, CA). Sections were then mounted onto slides with Vectashield (Vector).

For the silver-intensified immunogold reaction procedure (Dalezios et al. 2002), the monoclonal mouse antibody to Cx36 (1:500) and 2 different rabbit antibodies directed against the α1-GABA$_A$R subunit were used; one was directed to amino acid sequence 1–9 of the mature subunit located in the N-terminal part of the subunit and the other to amino acid sequence 328–382 of the mature subunit located in the cytoplasmic loop between the transmembrane region TM3 and TM4 (see Table 1). To increase the penetration of the reagents, sections were immersed in 10% (1 h), 20% (1–2 h), and 30% (overnight) sucrose in PB for cryoprotection then quickly frozen in liquid nitrogen and thawed in PB only for the reaction to reveal α1-GABA$_A$R. Floating sections were incubated for 1 h in 20% normal goat serum diluted in TBS. Sections were then incubated overnight with primary antibodies in TBS containing 1% normal serum (Table 1). Sections were incubated subsequently overnight at 4 °C in goat anti-mouse (Fab fragment) or anti-rabbit immunoglobulin G (IgG) coupled to 1.4 nm gold (Nanoprobes Inc., Stony Brook, NY) and made up in TBS containing 1% normal serum. After several washes in TBS, the sections were washed in double-distilled water, followed by silver enhancement of the gold particles with an HQ silver kit (Nanoprobes) for 8–12 min. Sections were then treated with 1% OsO$_4$, contrasted with 1% uranyl acetate, dehydrated, and embedded in epoxy resin (Durcupan ACM, Fluca, Sigma-Aldrich, Gillingham, UK). Ultrathin (70–80 nm thick) serial sections were collected on pioloform-coated copper grids, lead stained, and examined with an electron microscope.

References for the specificity of primary antibodies are given in Table 1. In addition, we have carried out tests for the specificity of antibodies to α1-GABA$_A$R using the brain of mice lacking α1-GABA$_A$R (Sur et al. 2001). The tissue was donated by Drs D. Belleli and J. Lambert at the Neurosciences Institute, University of Dundee. Wild-type littermate mice showed strong immunoreactivity of the brain, but the α1-GABA$_A$R-deficient mouse brains were completely devoid of immunofluorescence, providing evidence that these antibodies recognize α1-GABA$_A$R. Immunofluorescence testing of the monoclonal antibody to Cx36 in mice (Degen et al. 2004) lacking Cx36 expression (fixed brains kindly provided by Drs Joachim Degen and Klaus Willecke, Institute of Genetics, University of Bonn, Germany) showed that the frequency of immunoreactive dots, corresponding to gap junctions, was greatly reduced throughout the brain, but the dots were present in wild-type mice. The immunoreactivity of the brain of a Cx36-deficient mouse reacted for Cx43 was similar to that of the wild-type mouse (rabbit antibody, Code 71-0700, 1:1000, Zymed, San Francisco, CA).

Table 1
Summary of antibodies, their dilutions, and sources

Primary antibody to	Species	Dilution	Source of primary antibody	Characterization
PV	Guinea pig	1:1000	K.G. Baimbridge, University of British Columbia, Canada	Mithani et al. 1987
SOM	Mouse	1:500	A. Buchan, MRC Regulatory Peptide Group, Canada	Vincent et al. 1985
Cx36	Mouse	1:500	Chemicon www.chemicon.com	see Materials and Methods for ko test
GABA$_A$ α1 (N-terminus)	Rabbit	1:500	W. Sieghart, Center for Brain Research, Vienna, Austria	Zezula et al. 1991; see Materials and Methods for ko test
GABA$_A$ α1 (loop)	Rabbit	1:500	W. Sieghart, Center for Brain Research, Vienna, Austria	Tretter et al. 1997

To test cross-reactivity between various antibodies in double and triple immunolabeling experiments, sections were processed with a full complement of secondary antibodies and one primary antibody at a time. None of the combinations with species-unrelated secondary antibodies resulted in labeling. No selective labeling was found in sections incubated with combinations of secondary antibodies without a primary antibody.

Peroxidase Reactions

Peroxidase reactions for light and electron microscopy were performed as described previously (Maccaferri et al. 2000; Losonczy et al. 2002). Sections dedicated for electron microscopy were not used for immunofluorescence experiments previously, but were freeze/thawed, and no Triton was used in the buffer. Following evaluation of immunofluorescence, the sections containing recorded cells were reacted by avidin–biotinylated horse radish peroxidase (HRP) complex (Vector) followed by peroxidase reaction using diaminobenzidine (0.05%) as chromogen and H_2O_2 as substrate produced in situ as a glucose oxidase reaction product. To confirm that Cx36-immunopositive dots were indeed gap junctions, immunoperoxidase reaction was carried out, but the freeze-thawing step was omitted. The primary antibody (1:500) was followed by washing in TBS, biotinylated goat anti-mouse IgG (1:100, Vector), and avidin–biotinylated peroxidase complex (1:100, ABC Elite, Vector). Peroxidase reaction was carried out with diaminobenzidine (0.05%) as chromogen and 0.01% H_2O_2 as substrate.

After washing, the sections were treated with 1% OsO_4, 1% uranyl acetate in 70% ethanol, dehydrated, embedded in epoxy resin (Durcupan ACM, Fluca, Sigma-Aldrich), and mounted in Durcupan between slide and coverslip. For axoaxonic cells, axon-rich areas were cut out from the thin layer of resin on the slide and reembedded for ultrathin sectioning. Serial ultrathin sections were cut and mounted on single-slot, pioloform-coated copper grids, and synapses of filled boutons were sampled randomly with an electron microscope.

Image Acquisition and Analysis

Expression of the GABA$_A$ α1 subunit immunoreactivity in the dendrites of neurobiotin-filled cells was evaluated using a Zeiss LSM 510/Axiovert 100 M confocal microscope with a 63× oil lens at 1.5× digital zoom. Channel settings were as described earlier (Somogyi et al. 2004) and used the 488 nm band of an Ar laser to detect the fluorophore Alexa fluor-488 and the 543 and 633 nm bands of 2 HeNe lasers to detect the fluorophores Cy3 or Cy5, respectively. Images were acquired in sequential scan mode. Each scan of neurobiotin-filled dendrites was decomposed and saved as 3 separate images corresponding to each of the 3 channels. Evaluation of α1-GABA$_A$R immunoreactivity was performed using the public domain National Institutes of Health Image program (Scion Image, developed at the US National Institutes of Health, http://rsb.info.nih.gov/nih-image/). The 2 images of one single scan corresponding to α1-GABA$_A$R (channel 2) and to the neurobiotin labeling (channel 1) were restacked. The area of neurobiotin-filled dendrite was manually selected on channel 1 image, and the GABA$_A$ α1-IR (GABA$_A$ α1-immunoreactivity) was quantified by measuring the average gray value of the corresponding area on channel 2 image. The average gray value corresponds to the sum of the gray values of all the pixels in the selection divided by the number of pixels. The average gray value was calculated on each channel 2 image for the filled dendrites and for at least 3 neighboring unfilled but highly α1-GABA$_A$R–immunoreactive dendrites, which were used as an internal standard. For each filled dendrite, the ratio of the average gray values of the filled dendrite to the mean of the average gray values of at least 3 unfilled GABA$_A$ α1-IR dendrites was calculated and used as a metric for the characterization of the filled dendrite. Values for 2-12 scanned dendrites were averaged for each filled cell. The axoaxonic cells ($n = 4$), basket cells ($n = 4$), and bistratified cells ($n = 4$) were then compared.

Estimation of the number of PV-positive cells coexpressing immunoreactivity for α1-GABA$_A$R and for SOM and the relative amount of Cx36-immunopositive dots associated with PV-expressing dendrites was carried out in the CA1 area using a Leitz DM RB epifluorescence microscope with the filter sets described earlier (Ferraguti et al. 2004). For the estimation of the number of distinct PV-positive cells, the pyramidal layer was scanned using a 40× objective and every PV-positive

cell was recorded until a sample of 39–40 cells was reached. Coimmunoreactivity of a PV-positive cell for SOM indicated a putative bistratified cell. The cells were scored as either strongly or weakly α1-GABA$_A$R immunoreactive corresponding to putative basket or axoaxonic cells, respectively, by visual comparison of the dendritic α1-GABA$_A$R immunoreactivity of the PV-positive cells with the immunoreactivity of strongly labeled dendrites in the same field of view. For the quantification of the relative amount of Cx36-immunopositive dots associated with PV-expressing dendrites, all Cx36-immunopositive dots in an area of the dorsal CA1 region were photographed and evaluated to determine whether they were associated with PV-expressing dendrites. Strata radiatum and lacunosum-moleculare were sampled separately from stratum oriens. Sampling continued until about 40 dots were analyzed in each area of each section. A total of 3 sections from 3 different animals were evaluated. Images were recorded with a CCD camera (Hamamatsu C4742-95). The stored digital images were visualized and analyzed with Improvision software (Openlab, version 3.0.2; Improvision Ltd., www.improvision.com).

Results

In Vivo Labeling of Identified Axoaxonic, Basket, and Bistratified Cells

We labeled single axoaxonic, basket, and bistratified cells in the CA1 area of the hippocampus in anesthetized rats and subsequently determined their immunoreactivity for α1-GABA$_A$R, the neuropeptide SOM, and the gap junction–forming protein Cx36. We used the axonal and dendritic distribution, the postsynaptic target specificity, molecular expression patterns, and in vivo spike timing to confirm the identity of the recorded cells. In vivo firing patterns, axonal distribution, and PV expression of 3 cells used for this study have been presented previously in Klausberger et al. (2003) (axoaxonic cell T88a; basket cells T75aa, T80b).

The 5 labeled axoaxonic cells (T88a, T101d, T103b, T141a, T151b) had their soma close or within stratum pyramidale with dendrites stretching radially in strata radiatum and oriens and branching in stratum lacunosum-moleculare and alveus. Their terminal axons remained preferentially within the part of stratum pyramidale that borders stratum oriens (Fig. 1A1). To confirm the identity of the cells, we randomly sampled axonal boutons of the 4 newly filled cells in the electron microscope and identified the postsynaptic targets. Identified synaptic targets of cells T101d ($n = 14$), T103b ($n = 12$), and T141a ($n = 12$) were exclusively axon initial segments of pyramidal cells (Fig. 1B,C). For 2 of the cells (T101d and T141a), the postsynaptic targets of one bouton (of $n = 14$ and $n = 12$ studied, respectively) could not be identified, although the boutons clearly established type 2 synapses. Most of the recovered boutons (86%; $n = 22$) of cell T151b targeted initial segments, and the cell was therefore classified as axoaxonic cell, albeit 2 somata and a proximal dendrite of pyramidal cells were also found in the random sample of targets. The postsynaptic targets of axoaxonic cell T88a have been published previously (Klausberger et al. 2003). Axon initial segments were characterized by the presence of membrane undercoating and cisternal organelles. The firing patterns recorded in vivo were characteristic of axoaxonic cells as reported previously (Klausberger et al. 2003). The cells fired rhythmically around the positive peak of the theta oscillations recorded extracellularly in stratum pyramidale (Fig. 1E), and at the beginning of ripple episodes, but were silent subsequently (Fig. 1D).

The somata of basket cells (T75aa, T80b, T119a, T135b, T158b, C3a) were located in or close to stratum pyramidale
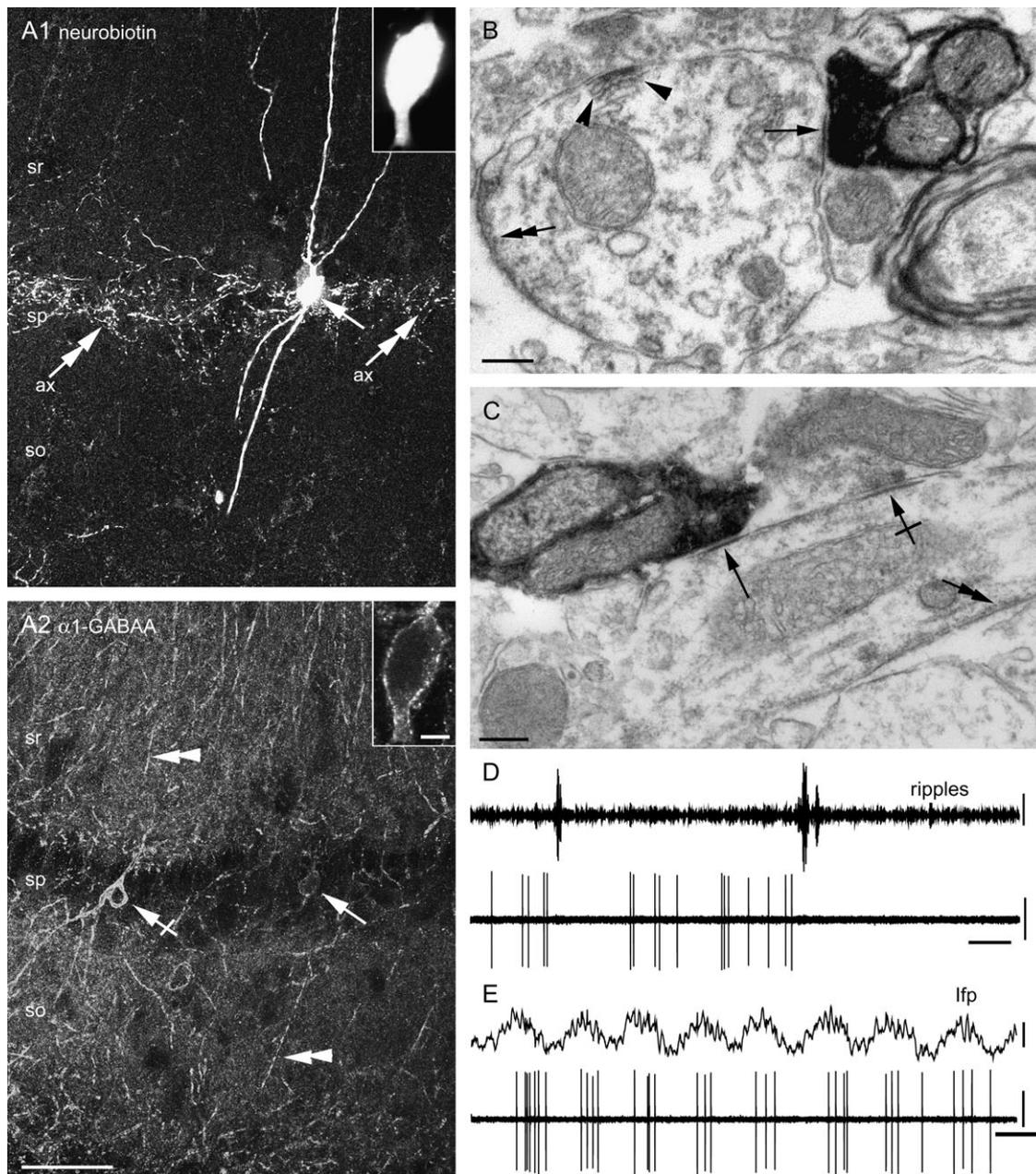
Figure 1. Expression of α1-GABA$_A$R and in vivo firing patterns of identified axoaxonic cells. (A) Confocal microscopic images of a 60-μm-thick section containing a (A1) neurobiotin-filled axoaxonic cell (T101d) immunoreacted (A2) for α1-GABA$_A$R. The soma of the cell (arrow in A1) is located in stratum pyramidale (sp), the dendrites extend radially in strata oriens (so), and radiatum (sr); the axon (double arrows) innervates stratum pyramidale and adjacent stratum oriens. Immunoreactivity for α1-GABA$_A$R shows both a relatively weak and diffuse labeling and a strong immunoreactivity on some interneuron dendrites (double arrowheads) and somata (e.g., crossed arrow). Insets and arrows in (A) demonstrate that the soma of the labeled cell is immunoreactive for α1-GABA$_A$R. (B,C) Electron micrographs of horseradish peroxidase product–labeled boutons of 2 different axoaxonic cells (T103b in B, T151b in C) in stratum pyramidale. The boutons make type 2 synapses (arrows) on axon initial segments identified by the presence of membrane undercoating (double arrows) and a cisternal organelle (arrowheads). Note the presence in (C) of an unfilled bouton establishing a type 2 synapse (crossed arrow). (D) The axoaxonic cell T101d fired before but was silent during and after ripple episodes recorded in an anesthetized rat. (E) The cell fired at the peak of theta oscillations recorded extracellularly in stratum pyramidale. Scale bars: (A1,2) 50 μm; insets 5 μm; (C,B) 0.2 μm; ripples 0.1 mV and 0.5 s; local field potential (lfp) 0.5 mV and 0.2 s; spikes 0.5 mV and 0.5 s in D, 0.2 s in E.

with dendrites branching mainly in the strata oriens and radiatum. Axonal arborizations were found mainly in stratum pyramidale but extended to different degrees into neighboring layers (Fig. 2A1). The cells fired rhythmically on the descending phase of theta oscillations (Fig. 2A3, bottom trace) and with high frequency at the troughs of sharp wave–associated ripples (Fig. 2A3, upper trace), as previously described in Klausberger et al. (2003).

Bistratified cells (T115b, T147b, C8b, C22a) had their soma in stratum pyramidale or adjacent stratum oriens with dendrites branching radially in strata oriens and radiatum but avoiding lacunosum-moleculare (Fig. 2B1). The cells fired rhythmically on the trough of the theta oscillations (Fig. 2B3, bottom trace) and at high frequency throughout the whole ripple episodes (Fig. 2B3, upper trace), as previously demonstrated (Klausberger et al. 2004).
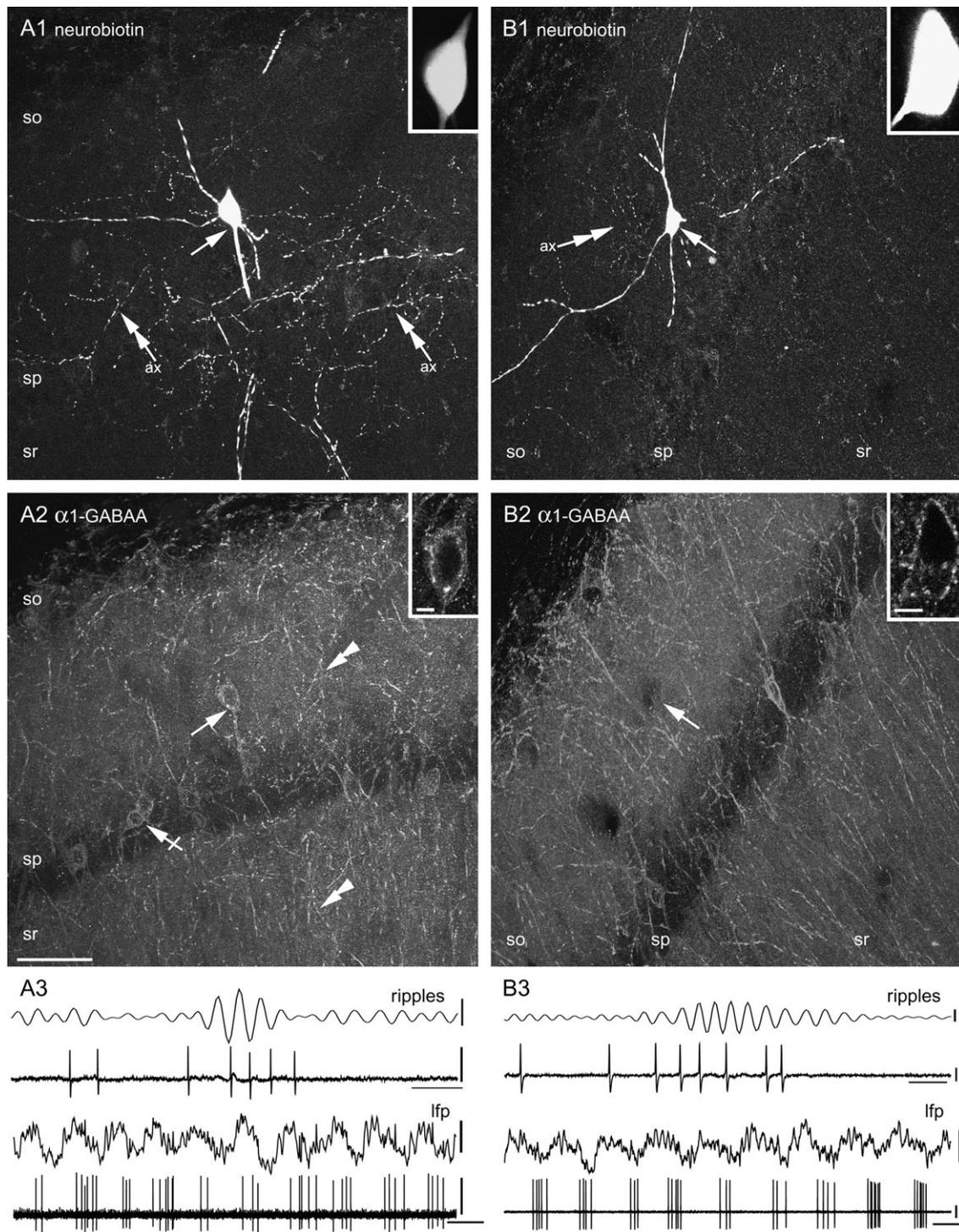
Figure 2. Immunoreactivity for α1-GABA$_A$R and in vivo firing patterns of identified basket and bistratified cells. (*A1–2, B1–2*) Confocal microscopic images of 60-μm-thick sections containing the somata of neurobiotin-labeled basket (T119a, *A1*) and bistratified (C8b, *B1*) cells, immunoreacted for α1-GABA$_A$R (*A2, B2*). The soma of the basket cell (arrow in *A1*) is located at the border between strata pyramidale (sp) and oriens (so), the dendrites arborize in strata oriens and radiatum (sr), and the axon branches mostly in stratum pyramidale (double arrows). The soma of the bistratified cell (arrow in *B1*) is located in stratum oriens with dendrites and the axon (e.g., double arrow) arborizing in strata oriens and radiatum. Strongly α1-GABA$_A$R–immunoreactive dendrites (e.g., double arrowheads) and somata (e.g., crossed arrow) are also present. Insets and arrows in (*A*) and (*B*) demonstrate that the soma of the labeled cells are immunoreactive for α1-GABA$_A$R. (*A3,B3*) Firing patterns of identified basket cell T119a and bistratified cell C8b during theta and ripple oscillations. Scale bars: (*A, B*) 50 μm; insets 5 μm; ripples 0.1 mV and 0.02 s; lfp 0.5 mV and 0.2 s; spikes 0.5 mV.

Differential Expression of the α1-GABA$_A$R in Axoaxonic, Basket, and Bistratified Cells

Using antibodies against α1-GABA$_A$R, we observed a diffuse immunoreactivity in the neuropil in strata oriens, radiatum and lacunosum-moleculare. In addition, the somatic and dendritic membranes of certain interneurons were very strongly labeled (Figs 1*A2* and 2*A2,B2*). Because some of these strongly immunoreactive interneurons were reported previously to be

PV positive (Gao and Fritschy 1994), we tested the $\alpha1$-GABA$_A$R immunoreactivity of identified axoaxonic, basket, and bistratified cells. All 3 types of cell expressed $\alpha1$-GABA$_A$R along their somatic membrane (Figs 1A and 2A,B), but we observed a differential expression along their dendritic membranes. Basket

(Fig. 3C) and bistratified (Fig. 3D) cells strongly expressed $\alpha1$-GABA$_A$R on their dendrites similar to other strongly immunoreactive dendrites in the field of view. However, dendrites of axoaxonic cells expressed $\alpha1$-GABA$_A$R to a much lesser extent than other strongly immunoreactive dendrites in the same field
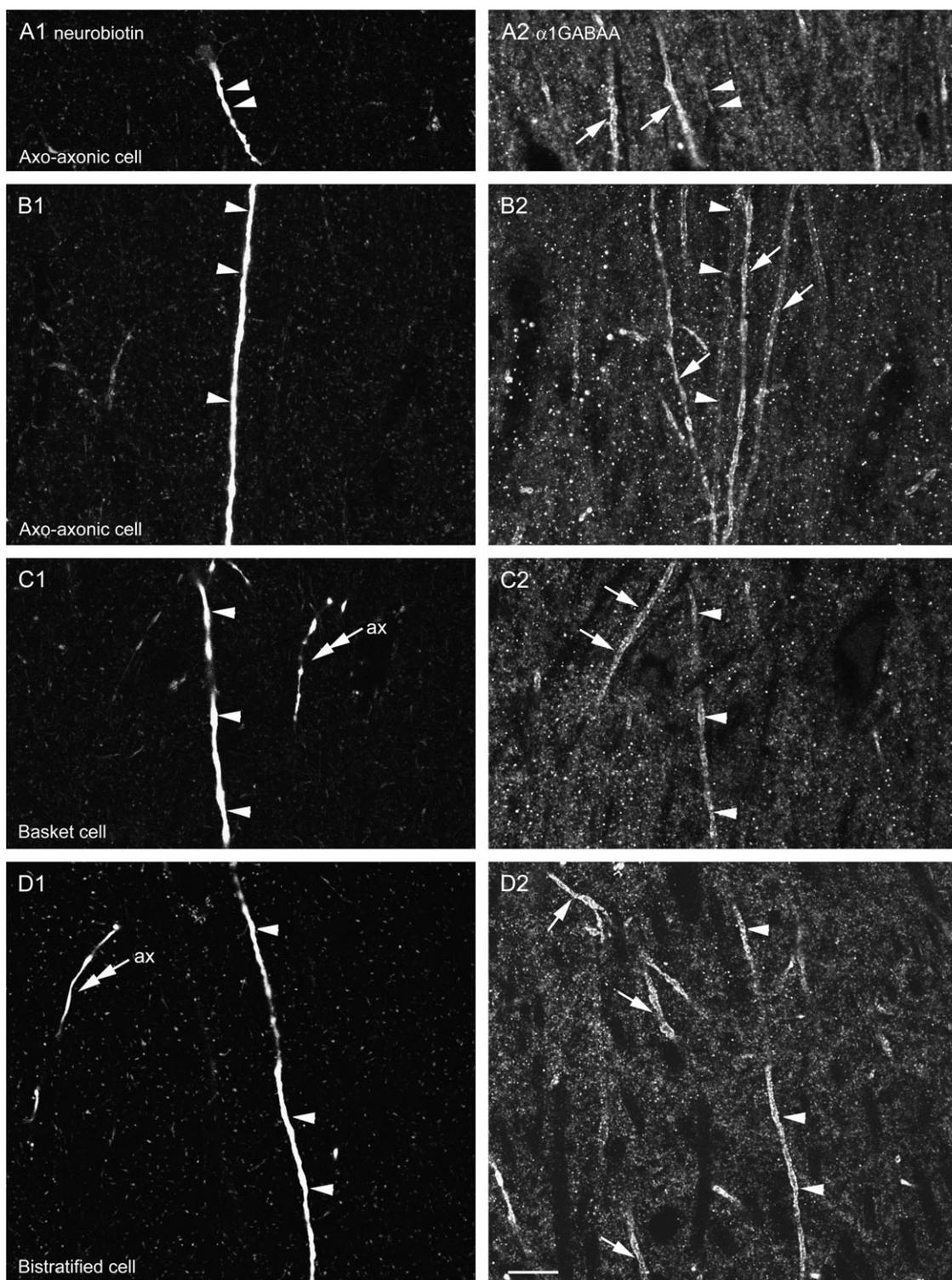
Figure 3. Confocal microscopic images of dendrites of axoaxonic, basket, and bistratified cells immunoreactive for $\alpha1$-GABA$_A$R. (A, B) Dendrites of 2 axoaxonic cells (T101d, T103b) exhibit weaker $\alpha1$-GABA$_A$R immunoreactivity (arrow heads) than neighboring strongly immunopositive dendrites of nonlabeled cells (arrows in A2, B2). (C, D) The dendrites of basket cell T119a (C1, C2) and bistratified cell C22a (D1, D2) are strongly immunopositive for $\alpha1$-GABA$_A$R similarly to other strongly labeled dendrites in the same field (arrow heads). Some axons of the labeled cells are also visible (ax, double arrows). Scale bar: 10 μm.

(Fig. 3A,B). To quantify dendritic immunoreactivity, we measured the mean gray density of α1-GABA$_A$R immunoreactivity of neurobiotin-filled dendrites of axoaxonic, basket, and bistratified cells and also the mean gray density of at least 3 strongly α1-GABA$_A$R–expressing dendrites in the same field of view in confocal images (arrows in Fig. 3A2–D2). We calculated the ratio between the gray densities of each neurobiotin-filled dendrite and the mean of the strongly immunoreactive dendrites not labeled by neurobiotin. For each labeled cell, 2–12 dendrites were measured, and the mean of the ratios for the different cells are presented in Table 2.

For the statistical evaluation of our data, we use a software for exact nonparametric inference (StatXact 7; www.cytel.com). The ratios for the 3 cell classes were significantly different (Kruskal–Wallis test, exact $P = 0.029$; Fig. 4), and post hoc Dunn test showed that the immunoreactivity ratios of axoaxonic cells ($n = 4$) were significantly different from basket ($n = 4$) and bistratified cells ($n = 4$) ($P < 0.05$); there was no difference between basket and bistratified cells ($P > 0.05$). This result demonstrated that the dendrites of axoaxonic cells express significantly less α1-GABA$_A$R than basket and bistratified cells. As a comparison, we labeled 3 pyramidal cells in vivo and tested their dendrites for α1-GABA$_A$R immunoreactivity. The ratios of their α1-GABA$_A$R immunoreactivity in comparison with strongly immunoreactive dendrites in the same field of view were 0.31, 0.50, and 0.42. Their mean immunoreactivity was significantly lower than the ratios obtained for axoaxonic cells (permutation test, exact $P = 0.0286$).

Extrasynaptic Distribution of the α1-GABA$_A$R in Interneurons

The continuous distribution of strong α1-GABA$_A$R immunoreactivity along the membranes of somata and dendrites of interneurons (Figs 1A2, 2A2,B2, and 5A–D) suggests a high level of extrasynaptically located GABA$_A$ receptors containing α1 subunits in these cells and therefore could be the source of the strong tonic inhibition described in fast-spiking cells (Semyanov et al. 2003). To examine this, we used a preembedding silver-intensified immunogold reaction and found that antibodies against α1-GABA$_A$R strongly labeled the extrasynaptic plasma membrane of somata and dendrites of interneurons (Fig. 5E–I). Silver/gold particles were also found at the edges of type 1 and type 2 synapses (Fig. 5I), but no immunoreactivity was found in axons or axon terminals. The apparent absence of synaptic labeling can be explained by the lack of penetration of the gold-coupled antibody into the synaptic cleft or postsynaptic specialization using the preembedding method on tissue not treated with a detergent. A similar lack of synaptic

labeling of GABA$_A$ receptor subunits with this method has been reported before (Nusser, Roberts, Baude, Richards, Sieghart, et al. 1995). The labeling patterns obtained with 2 different antibodies directed against either the intracellular loop (Fig. 5A,B,E,F) or the extracellular N-terminus (Fig. 5C,D,G,H,I) of the α1 subunit were similar and suggested a strong extrasynaptic expression of α1-GABA$_A$R on the dendritic membrane of interneurons.

Differential Expression of the Neuropeptide Somatostatin in Axoaxonic, Basket, and Bistratified Cells

We have reported previously that bistratified cells express the neuropeptide SOM (Klausberger et al. 2004). Because of the relatively small number of SOM-positive cells in the pyramidal cell layer (Jinno and Kosaka 2000), it has been generally assumed that basket and axoaxonic cells do not express SOM, but, to our knowledge, this has not been tested directly. Therefore, we reacted sections including the somata of identified PV-expressing basket and axoaxonic cells using immunofluorescence (Fig. 6). All 3 tested basket (T80b, T119a, T158b) and all 3 tested axoaxonic cells (T101d, T103b, T151b) were immunonegative for SOM, although other interneurons in the pyramidal cell layer were positive for SOM in the same section.

Estimation of the Proportion of Axoaxonic, Basket, and Bistratified Cells in the Pyramidal Cell Layer of the CA1 Area

We performed triple-immunofluorescence labeling with antibodies against PV, α1-GABA$_A$R, and SOM on sections from 3 different rats to estimate the relative numbers of axoaxonic, basket, and bistratified cells in the pyramidal cell layer. First, we photographed each PV-positive cell in the pyramidal cell layer. If the cell was also immunoreactive for SOM, it was identified as a putative bistratified cell. If the cell was immunonegative for SOM, its dendrites were tested for α1-GABA$_A$R immunoreactivity and compared visually with the immunoreactivity of strongly labeled dendrites in the same field of view. The cells were scored as either strongly or weakly α1-GABA$_A$R immunoreactive corresponding to putative basket or axoaxonic cells, respectively. No difference was found between the relative number of cells from 3 animals (Kruskall–Wallis test, exact $P = 1$; respectively in each animal, for axoaxonic cells $n = 7, 5, 7$; for basket cells $n = 24, 25, 23$; for bistratified cells $n = 9, 10, 9$), and the data were pooled. The results indicated that the largest population of PV-positive cells in the pyramidal cell layer are likely to be basket cells (60%), whereas bistratified (24%) and axoaxonic (16%) cells form smaller populations (Fig. 7).

Table 2

Quantification of the α1-GABA$_A$R immunoreactivity of in vivo labeled axoaxonic, basket, and bistratified cell dendrites

Axoaxonic cells		Basket cells		Bistratified cells	
Cell number	α1-GABA$_A$R-IR (Mean ± SEM)	Cell number	α1-GABA$_A$R-IR (Mean ± SEM)	Cell number	α1-GABA$_A$R-IR (Mean ± SEM)
T101d	0.55 ± 0.043 ($n = 12$)	C3a	0.61 ± 0.082 ($n = 2$)	T115b	0.93 ± 0.029 ($n = 5$)
T103b	0.54 ± 0.056 ($n = 15$)	T75aa	0.99 ± 0.086 ($n = 2$)	C8b	0.73 ± 0.084 ($n = 7$)
T88a	0.69 ± 0.141 ($n = 7$)	T119a	0.85 ± 0.167 ($n = 8$)	C22a	0.78 ± 0.052 ($n = 8$)
T151b	0.59 ± 0.045 ($n = 3$)	T135b	0.82 ± 0.104 ($n = 7$)	T147b	0.98 ± 0.236 ($n = 2$)

Note: Immunoreactivity for the α1 subunit (α1-GABA$_A$R-IR) is given as the mean for each cell of the ratios between the α1-GABA$_A$R immunoreactivity measured in confocal images as the mean gray density of each labeled dendrite and the mean of gray density of at least 3 strongly α1-GABA$_A$R–immunoreactive neighboring dendrites in the same field of view. $n =$ number of filled dendrites tested for each cell. SEM, standard error of mean.
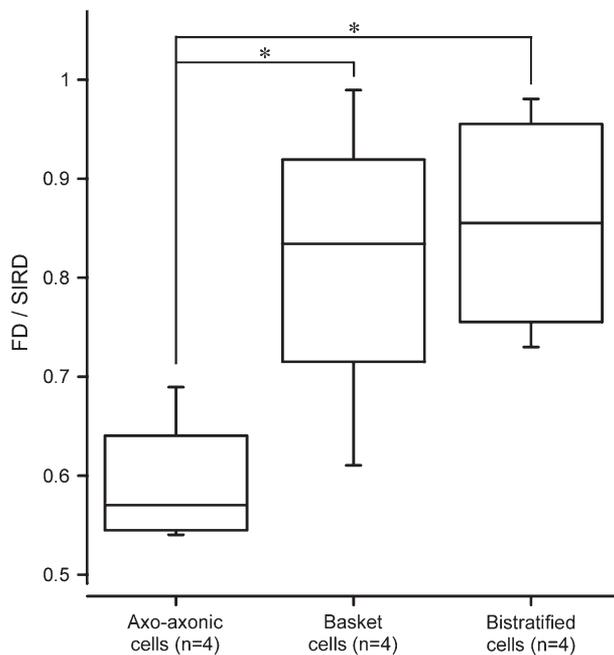
Figure 4. Differential expression of α1-GABA$_A$R in identified axoaxonic, basket, and bistratified cells measured in confocal microscopic images. Axoaxonic cell dendrites exhibit significantly less immunoreactivity for α1-GABA$_A$R than basket and bistratified cell dendrites. No difference is found between basket and bistratified cell dendrites. Immunoreactivity for each cell was calculated as the mean ratio between the α1-GABA$_A$R immunoreactivity of 2–12 neurobiotin-filled dendrites (FD) and the mean of 3 or more strongly α1-GABA$_A$R–immunoreactive neighboring dendrites (SIRD) in the same field of view. Each box encloses 50% of the data. The top and bottom of the box mark the limits of ±25% of the sample, and the median value is displayed as a line. The lines extending from the top and bottom of each box mark the minimum and maximum values within the sample.

Cx36 Immunoreactivity at Dendritic Junctions of Axoaxonic, Bistratified, and PV Cells

Immunofluorescence labeling with antibodies against Cx36 resulted in dotty labeling in the CA1 area. The most prominent labeling was found in stratum radiatum toward stratum lacunosum-moleculare and in stratum lacunosum-moleculare and at the border between stratum oriens and alveus. When immunolabeling for Cx36 was combined with PV immunocytochemistry, most of the Cx36-positive dots were colocalized with PV-positive dendrites (Fig. 8A). Counts in 3 animals show that 76 ± 7% (mean ± standard deviation) of Cx36-positive dots ($n = 249$) were associated with the crossings of 2 PV-expressing dendrites, 18 ± 8% were associated with a single PV-expressing dendrites, and 6 ± 2% were not associated with PV-expressing processes. No significant differences were found for the distributions in stratum radiatum/lacunosum-moleculare versus stratum oriens in the 3 animals ($P > 0.2$, χ^2 test).

To test if the dots correspond to gap junctions, 4 silver-intensified, immunogold-labeled dots in stratum radiatum (Fig. 8Ba) and 2 immunoperoxidase-labeled dots in stratum oriens were analyzed in the electron microscope. After appropriate tilting of the sections, we could show that all 6 dots were dendrodendritic gap junctions as evidenced by the close apposition of the 2 plasma membranes and the presence of the gap that was filled with electron opaque peroxidase product (Fig. 8Bb). The silver particles were lined up along the cytoplasmic face of the junctions.

We tested the Cx36 immunoreactivity of neurobiotin-filled cells and found Cx36-immunopositive dots at junctions between dendrites of axoaxonic ($n = 3$), basket ($n = 1$), and bistratified ($n = 2$) cells and unfilled PV- or α1-GABA$_A$R–immunoreactive dendrites (Fig. 8C–F). In addition, we found that dendrites of the filled axoaxonic cell T88a (Fig. 8D), which were weakly immunopositive for α1-GABA$_A$R, shared Cx36 labeling with strongly α1-GABA$_A$R–immunoreactive dendrites. This suggests that axoaxonic cells may establish gap junctions also with other types of interneurons. Overall, these results indicate that basket, bistratified, and axoaxonic cells form Cx36-immunopositive dendrodendritic gap junctions.

Discussion

Relative Frequencies of Basket, Bistratified, and Axoaxonic Cells

PV-expressing axoaxonic, basket, and bistratified cells are distinct cell types, releasing GABA to different domains of postsynaptic pyramidal cells at different temporal phases of theta oscillations and also behaving differently during high-frequency sharp wave–associated ripple oscillations (Klausberger et al. 2003, 2004). We have demonstrated that these 3 cell types can be distinguished on the basis of their differential molecular expression profile as well. Our results support that of the 3 cell types, only bistratified cells express the neuropeptide SOM. We have not found SOM immunoreactivity in axoaxonic and basket cell somata. Axoaxonic cells can be differentiated from basket and bistratified cells by the lower amount of GABA$_A$ receptor α1 subunit along their dendritic membrane. Using the molecular expression profile of different interneuron classes, we have estimated that in stratum pyramidale of the CA1 area, basket, bistratified, and axoaxonic cells represent 60%, 25%, and 15% of PV-containing cells, respectively. Intracellular recordings of 36 PV-immunoreactive cells in slices of adult rat hippocampus (Pawelzik et al. 2002) resulted in comparable proportions of the 3 cell types: 80% basket cells, 17% bistratified cells, and 4% axoaxonic cells. Differences between the 2 data sets may originate from the use of different methods and sample sizes. Previously, the fraction of interneurons expressing PV was estimated to represent 20% of all GABAergic cells in the dorsal hippocampus in the rat and mouse (Kosaka et al. 1987; Jinno and Kosaka 2002). Combining these data with our results, we can estimate that PV-containing basket, bistratified, and axoaxonic cells represent 12%, 5%, and 3%, respectively, of all GABAergic interneurons in the CA1 area. However, stratum oriens also contain significant numbers of PV-positive interneurons, and we have not been able to establish if they represent cell types in the same proportion as those in stratum pyramidale. At least one other cell type, the O-LM cell, also expresses PV, albeit at a lower level (Klausberger et al. 2003) than basket, axoaxonic, or bistratified cells. This cell type also expresses SOM, it is located in stratum oriens and, so far, has not been reported from stratum pyramidale in the rat (but see Oliva et al. 2000 in the mouse); therefore, it is unlikely that it contaminated our estimate of bistratified cells.

Extrasynaptic and Pathway-Preferential Expression of GABA$_A$ Receptor α1 Subunit

The results indicate that the high density of the α1-GABA$_A$Rs reported previously on hippocampal interneurons (Gao and Fritschy 1994; Nusser, Roberts, Baude, Richards, Sieghart, et al.
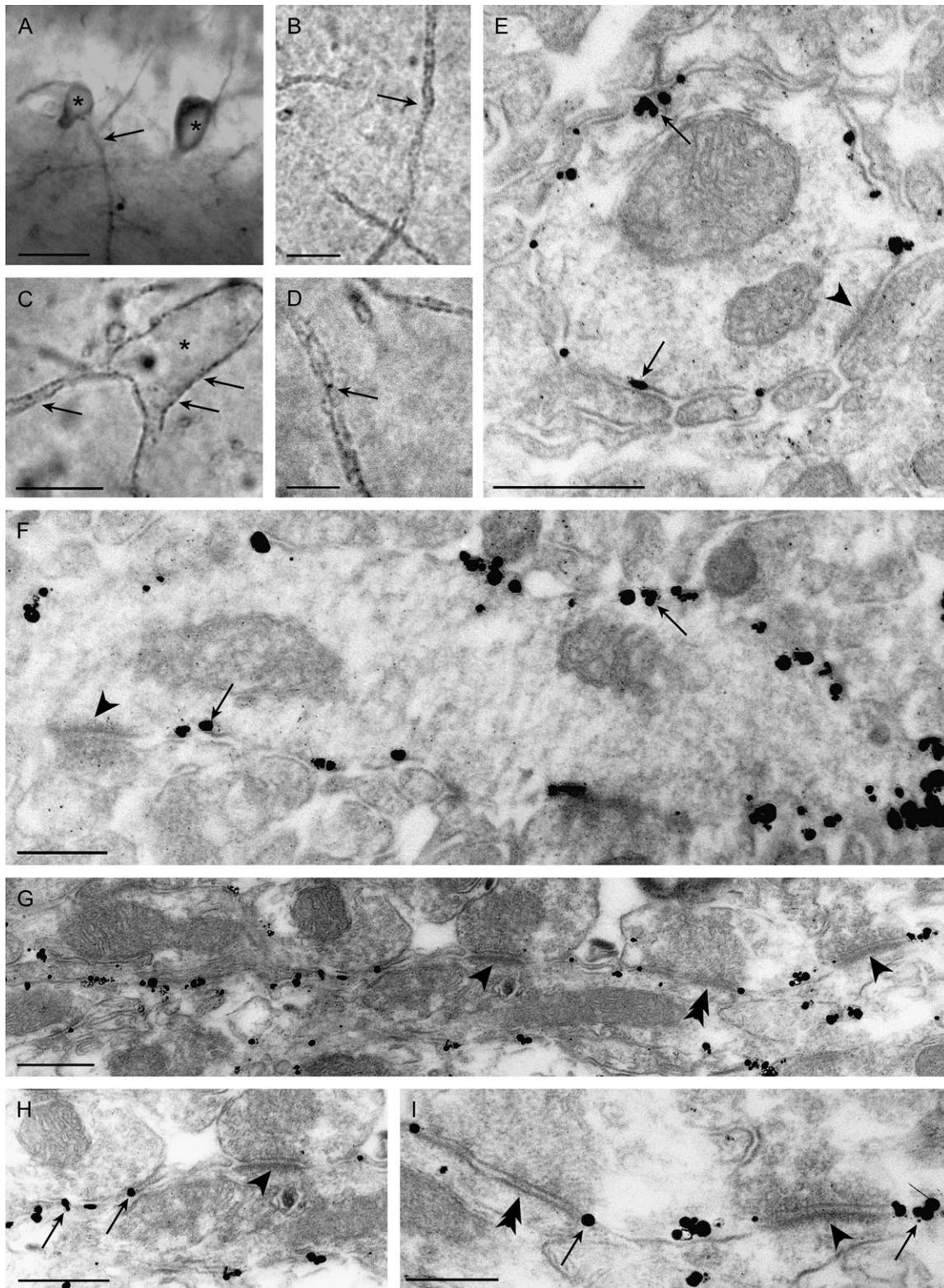
Figure 5. Extrasynaptic distribution of the α1-GABA$_A$R as demonstrated by preembedding silver-enhanced gold immunocytochemistry. (*A–D*) Light micrographs show strong α1-GABA$_A$R immunolabeling (arrows) distributed along the dendritic and somatic membranes of interneurons (stars). (*E–I*) Electron micrographs show that silver-enhanced gold particles (arrows) are densely distributed along the extrasynaptic membrane of interneuron dendrites avoiding both type 1 (arrow heads) and type 2 (double arrow heads) synapses, due to a lack of penetration of the gold-coupled antibody into the synaptic cleft. Dendrites in (*F*) and (*G*) originate from interneurons as they receive type 1 synapses (arrow heads) on their shaft. In (*A, B, E, F*), antibodies against the intracellular loop of the α1 subunit were used. In (*C, D, G, H*), antibodies against the extracellular *N*-terminus were used. Images (*H, I*) are enlargements of synapses shown in (*G*). Scale bars: (*A*) 20 µm, (*C*) 10 µm; (*B, D*) 5 µm; (*E, G*) 0.4um; (*F, H*) 0.3um; (*I*) 0.2um.
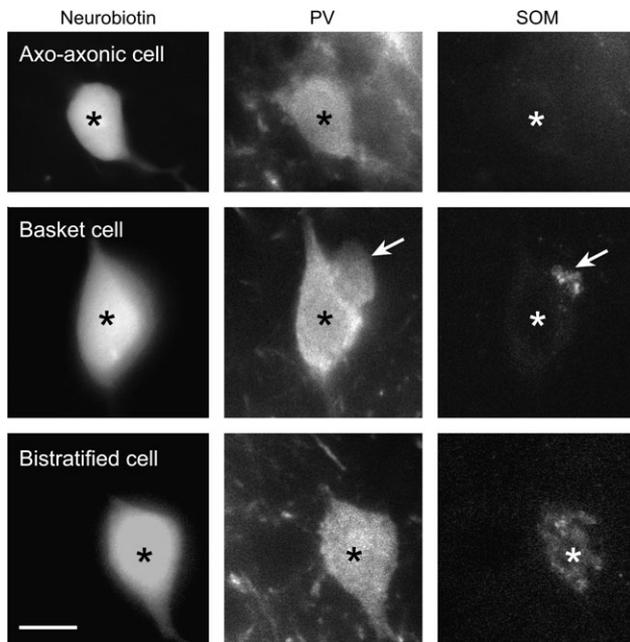
Figure 6. Triple-immunofluorescence micrographs testing the expression of PV and SOM in neurobiotin-filled axoaxonic, basket, and bistratified cells. The somata (stars) of all 3 cells are immunopositive for PV, but only the bistratified cell is positive for SOM. Note the part of the soma of an unfilled cell (arrows) expressing PV and SOM, which is apposed to the soma of the filled basket cell. Scale bar: 10 μm.
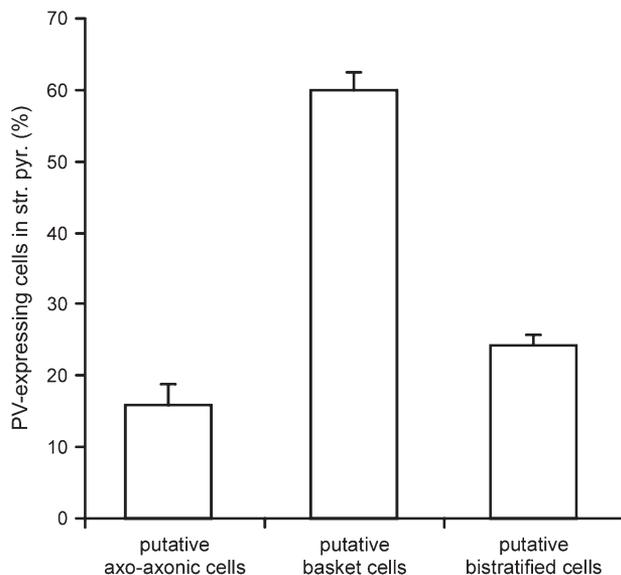

Figure 7. Estimation of the proportion of PV-expressing axoaxonic, basket, and bistratified cells in the pyramidal cell layer using triple immunofluorescence with antibodies to PV, α1-GABA$_A$R, and SOM. Each PV-positive cell in the pyramidal cell layer was photographed; immunoreactivity for SOM indicated a bistratified cell; visually scored weak or strong α1-GABA$_A$R immunoreactivity in SOM-negative cells indicated axoaxonic or basket cells, respectively. Data represent mean ± standard deviation from 3 different rats.

1995) is mostly expressed along the extrasynaptic plasma membrane of PV-expressing basket and bistratified cells. A similar high density of extrasynaptic receptors has been described in cerebellar granule cells; the total number of extrasynaptic GABA$_A$ receptors was estimated to exceed synaptic receptors (Nusser, Roberts, Baude, Richards, and Somogyi 1995) and suggested to mediate tonic inhibition (Kaneda et al. 1995;

Brickley et al. 1996). Comparable GABA$_A$ receptor–mediated tonic currents have been recorded in granule cells of the dentate gyrus (Nusser and Mody 2002) and in some hippocampal interneurons (Semyanov et al. 2003). The current carried by the tonic conductance can be larger than the time-averaged spontaneous inhibitory postsynaptic current (for review, see Semyanov et al. 2004; Farrant and Nusser 2005). Tonic GABA$_A$ receptor–mediated conductances in hippocampal interneurons were sensitive to the benzodiapine receptor agonist zolpidem (Semyanov et al. 2003). This is supported by the much higher amount of α1 subunit in the extrasynaptic membranes of interneurons as compared with pyramidal cells.

The relatively low number of extrasynaptic receptors on pyramidal cells indicates the dominance of phasic inhibition. In contrast, the high density of extrasynaptic receptors on some interneurons will result in an extracellular GABA concentration-dependent persistent increase in input conductance due to tonic inhibition (Semyanov et al. 2003; Farrant and Nusser 2005). Tonic inhibition reduces the size and duration of incoming excitatory postsynaptic potentials and the time window for signal integration, which might result in increased temporal precision of action potentials generated by the cells. Interestingly, PV-expressing basket and bistratified cells, expressing high amounts of extrasynaptic GABA$_A$ receptors, fire in a phase-modulated fashion during high-frequency sharp wave–associated ripples at millisecond precision (Klausberger et al. 2003, 2004). In contrast, axoaxonic cells that have significantly less extrasynaptic GABA$_A$ receptors along their dendritic membranes, stop firing during high-frequency ripples (Klausberger et al. 2003). Similarly, cholecystokinin (CCK)-expressing interneurons do not show high GABA$_A$ receptor immunoreactivity (Gao and Fritschy 1994) and fire relatively little during ripple oscillations (Klausberger et al. 2005). Therefore, it appears that in basket and bistratified cells, the very strong excitation from CA3 and CA1 pyramidal cells during ripples overcomes the strong tonic inhibition produced by extrasynaptic GABA$_A$ receptors, and this tonic inhibition is necessary to achieve their temporal precision of phase-related firing at frequencies above 100 Hz. This indicates that at least in the CA1 area of the hippocampus, tonic inhibition is not used by silent cells to achieve their hyperpolarized state but by the most active cells to achieve their high precision spike timing.

The α1-GABA$_A$Rs is not only expressed extracellularly by PV-expressing interneurons but also enriched in the synapses of pyramidal cells receiving input from PV-expressing basket and axoaxonic cells (Somogyi et al. 1996; Klausberger et al. 2002). In contrast, the axosomatic synapses established by CCK-expressing basket cells contain less α1 subunit– and more α2 subunit–containing GABA$_A$ receptors (Nusser et al. 1996; Pawelzik et al. 1999; Nyiri et al. 2001). The GABA$_A$ receptor subtypes in synapses of pyramidal cells receiving input from bistratified cells remain to be identified. Such an input pathway–dependent expression of distinct GABA$_A$ receptors could explain the different behavioral consequences of altering GABA$_A$ receptor subtypes (Rudolph et al. 1999; McKernan et al. 2000; Rudolph and Mohler 2006).

Cx36 Immunoreactivity in Dendrodendritic Gap Junctions of Axoaxonic, Basket, and Bistratified Cells

The presence of Cx36-immunoreactive spots at dendrodendritic alignments of the 3 identified PV-positive cell types strongly suggests that they are involved in electrical coupling
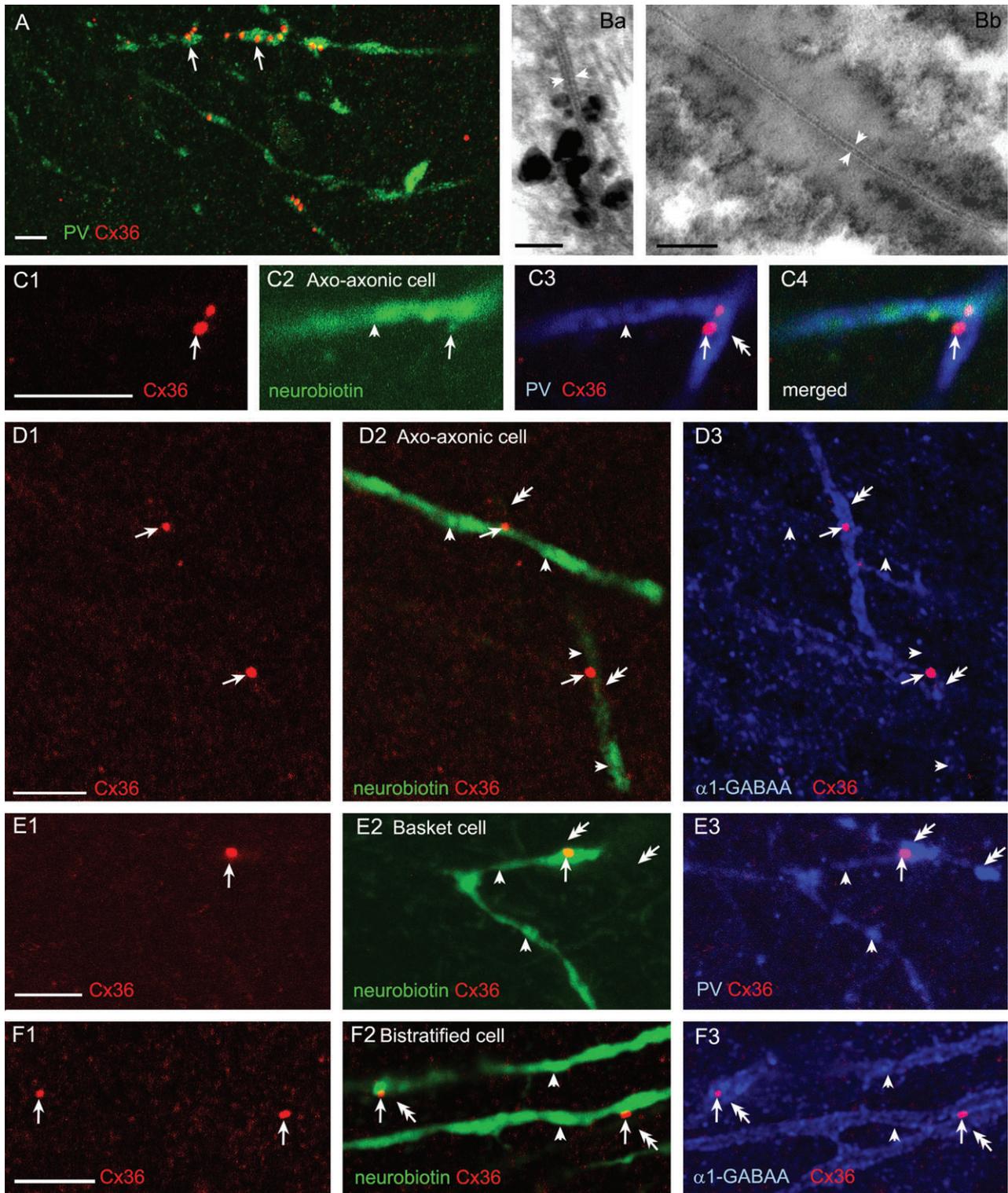
Figure 8. Axoaxonic, basket, and bistratified cells express Cx36-immunopositive clusters at dendritic junctions. (*A*) Confocal view of section immunoreacted for PV and Cx36 show that Cx36-immunoreactive dots (arrows) are strongly enriched at PV-positive dendrites. (*B*) Electron microscopic demonstration that immunopositive dots correspond to gap junctions using silver-intensified immunogold (*Ba*) or immunoperoxidase (*Bb*) reactions. The metal particles surround the gap junction (between white arrowheads) on the cytoplasmic side of a dendrodendritic gap junction in stratum radiatum. The peroxidase reaction product on the right covers the cytoplasmic sides of both closely apposed membranes as well as penetrates into the gap, leaving the 2 lipid bilayers as electron lucent parallel bands (between white arrowheads). (*C–F*) Confocal views of neurobiotin-filled dendrites (arrowheads) of axoaxonic (T103b, T88a), basket (T119a), and bistratified (C22a) cells expressing Cx36-immunoreactive dots (arrows) at junctions with dendrites of unfilled cells immunoreactive for PV and $\alpha1$-GABA$_A$R (double arrows). Note that in (*C1*), one of the Cx36-immunoreactive dots (arrow) is located on a spine emanating from the filled dendrite (arrow in *C2*). Axoaxonic cell T88a in (*D3*) expresses low amounts of $\alpha1$-GABA$_A$R but forms a Cx36-immunoreactive junction with a strongly $\alpha1$-GABA$_A$R–expressing dendrite, presumably originating from another type of cell. Arrowheads show that the dendrites of the filled cells are immunoreactive for PV (*C3*, *E3*) or $\alpha1$-GABA$_A$ (*D3*, *F3*). Scale bars: (*B*) 50 nm; (*A*, *C–F*) 5 µm.

via gap junctions, as shown by electron microscopy of PV-positive neurons previously (Fukuda and Kosaka 2003; Fukuda et al. 2006) and confirmed for the anti-Cx36 antibody with electron microscopy here. Many species of gap junction protein have been detected in the brain including the hippocampus (for review, see Connors and Long 2004; Sohl et al. 2004). Accordingly, Cx36 (Venance et al. 2000; Condorelli et al. 2003) as well as pannexin 1 and 2 (Bruzzone et al. 2003; Vogt et al. 2005) have been described in interneurons, but the expression of other gap junction–forming proteins cannot be excluded. In our material, most of the Cx36-immunolabeled dots overlapped with PV-positive dendrites in the hippocampus. Somatodendritic gap junctions have been described for PV-positive basket cells in the isocortex (Tamas et al. 2000). However, interneurons that do not express PV may also be coupled electrically (Gibson et al. 1999; Szabadics et al. 2001; Galarreta et al. 2004; Price et al. 2005; Zsiros and Maccaferri 2005). As most Cx36 immunolabeling was associated with PV neurons in the hippocampus, it is possible that different molecular species of connexin or pannexin are expressed by other types of GABAergic interneurons.

The presence of immunoreactivity for Cx36 at meeting points between dendrites of identified axoaxonic, basket, or bistratified cells and unidentified PV or α1-GABA$_A$R–immunoreactive dendrites is in line with reports of electrical coupling between interneurons of the same class (Galarreta and Hestrin 1999; Gibson et al. 1999; Tamas et al. 2000; Fukuda and Kosaka 2003; Price et al. 2005; Zsiros and Maccaferri 2005). This might be of particular importance for the synchronization of axoaxonic cells because no GABAergic synaptic input or interconnectivity has been reported between members of this cell type. However, in one case, an axoaxonic cell dendrite shared Cx36 immunolabeling with a strongly α1-GABA$_A$R–immunoreactive dendrite, suggesting the formation of a gap junction with a non-axoaxonic cell. Electrical coupling between neurons of different classes has been described rarely for fast-spiking cortical interneurons (Gibson et al. 1999) and more frequently for other interneurons (Simon et al. 2005). In addition, gap junctions between PV-positive and negative, presumptive interneuron dendrites have been also described in rat cortex (Fukuda and Kosaka 2003).

The role of gap junctions in the synchronization of neuronal activity, although intuitively obvious, remains a matter of debate (for review, see LeBeau et al. 2003; Whittington and Traub 2003; Hestrin and Galarreta 2005). In vitro recordings from Cx36 knockout mice indicated that Cx36-containing gap junctions contribute to various slow and high-frequency oscillations in the hippocampus (Hormuzdi et al. 2001) and in the cortex (Deans et al. 2001). However, in vivo recordings in the Cx36 knockout mice have shown that only gamma oscillations were impaired, but high-frequency ripple oscillations remained unchanged (Buhl et al. 2003). According to our results, deletion of Cx36 gene would affect mostly PV-expressing interneurons in the hippocampus. This is in line with the observation that basket and axoaxonic cells are strongly phase modulated during gamma oscillations in vitro (Hajos et al. 2004) and perisomatic inhibition seems to be the main force behind gamma oscillations in vitro (Mann et al. 2005). Overall, our data support the hypothesis that PV-expressing interneurons, including basket, axoaxonic, and bistratified cells, contribute to the generation and maintenance of gamma oscillations in the hippocampus with the involvement of Cx36-enriched gap junctions and α1 subunit–containing GABA$_A$ receptors.

References

Bartos M, Vida I, Frotscher M, Meyer A, Monyer H, Geiger JRP, Jonas P. 2002. Fast synaptic inhibition promotes synchronized gamma oscillations in hippocampal interneuron networks. Proc Natl Acad Sci USA. 99:13222-13227.

Baude A, Nusser Z, Roberts JDB, Mulvihill E, McIlhinney RAJ, Somogyi P. 1993. The metabotropic glutamate receptor (mGluR1a) is concentrated at perisynaptic membrane of neuronal subpopulations as detected by immunogold reaction. Neuron. 11:771-787.

Brickley SG, Cull-Candy SG, Farrant M. 1996. Development of a tonic form of synaptic inhibition in rat cerebellar granule cells resulting from persistent activation of GABAA receptors. J Physiol Lond. 497:753-759.

Bruzzone R, Hormuzdi SG, Barbe MT, Herb A, Monyer H. 2003. Pannexins, a family of gap junction proteins expressed in brain. Proc Natl Acad Sci USA. 100:13644-13649.

Buhl DL, Harris KD, Hormuzdi SG, Monyer H, Buzsaki G. 2003. Selective impairment of hippocampal gamma oscillations in connexin-36 knock-out mouse in vivo. J Neurosci. 23:1013-1018.

Condorelli DF, Trovato-Salinaro A, Mudo G, Mirone MB, Belluardo N. 2003. Cellular expression of connexins in the rat brain: neuronal localization, effects of kainate-induced seizures and expression in apoptotic neuronal cells. Eur J Neurosci. 18:1807-1827.

Connors BW, Long MA. 2004. Electrical synapses in the mammalian brain. Annu Rev Neurosci. 27:393-418.

Dalezios Y, Lujan R, Shigemoto R, Roberts JDB, Somogyi P. 2002. Enrichment of mGluR7a in the presynaptic active zones of GABAergic and non-GABAergic terminals on interneurons in the rat somatosensory cortex. Cereb Cortex. 12:961-974.

Deans MR, Gibson JR, Sellitto C, Connors BW, Paul DL. 2001. Synchronous activity of inhibitory networks in neocortex requires electrical synapses containing connexin36. Neuron. 31:477-485.

Degen J, Meier C, Van Der Giessen RS, Sohl G, Petrasch-Parwez E, Urschel S, Dermietzel R, Schilling K, De Zeeuw CI, Willecke K. 2004. Expression pattern of lacZ reporter gene representing connexin36 in transgenic mice. J Comp Neurol. 473:511-525.

Farrant M, Nusser Z. 2005. Variations on an inhibitory theme: phasic and tonic activation of GABA$_A$ receptors. Nat Rev Neurosci. 6:215-229.

Ferraguti F, Cobden P, Pollard M, Cope D, Shigemoto R, Watanabe M, Somogyi P. 2004. Immunolocalization of metabotropic glutamate receptor 1a (mGluR1α) in distinct classes of interneuron in the CA1 region of the rat hippocampus. Hippocampus. 14:193-215.

Freund TF, Buzsaki G. 1996. Interneurons of the hippocampus. Hippocampus. 6:347-470.

Fukuda T, Kosaka T. 2003. Ultrastructural study of gap junctions between dendrites of parvalbumin-containing gabaergic neurons in various neocortical areas of the adult rat. Neuroscience. 120:5-20.

Fukuda T, Kosaka T, Singer W, Galuske RAW. 2006. Gap junctions among dendrites of cortical GABAergic neurons establish a dense and widespread intercolumnar network. J Neurosci. 26:3434-3443.

Galarreta M, Erdélyi F, Szabó G, Hestrin S. 2004. Electrical coupling among irregular-spiking GABAergic interneurons expressing cannabinoid receptors. J Neurosci. 24:9770-9778.

Galarreta M, Hestrin S. 1999. A network of fast-spiking cells in the neocortex connected by electrical synapses. Nature. 402:72-75.

Gao B, Fritschy JM. 1994. Selective allocation of GABAA receptors containing the α1 subunit to neurochemically distinct sub-populations of rat hippocampal interneurons. Eur J Neurosci. 6: 837–853.

Gibson JR, Beierlein M, Connors BW. 1999. Two networks of electrically coupled inhibitory neurons in neocortex. Nature. 402:75–79.

Gonchar Y, Turney S, Price JL, Burkhalter A. 2002. Axo-axonic synapses formed by somatostatin-expressing GABAergic neurons in rat and monkey visual cortex. J Comp Neurol. 443:1–14.

Gulyas AL, Hajos N, Katona I, Freund TF. 2003. Interneurons are the local targets of hippocampal inhibitory cells which project to the medial septum. Eur J Neurosci. 17:1861–1872.

Hajos N, Palhalmi J, Mann EO, Nemeth B, Paulsen O, Freund TF. 2004. Spike timing of distinct types of GABAergic interneuron during hippocampal gamma oscillations in vitro. J Neurosci. 24:9127–9137.

Hestrin S, Galarreta M. 2005. Electrical synapses define networks of neocortical GABAergic neurons. Trends Neurosci. 28:304–309.

Hormuzdi SG, Pais I, LeBeau FEN, Towers SK, Rozov A, Buhl EH, Whittington MA, Monyer H. 2001. Impaired electrical signaling disrupts gamma frequency oscillations in connexin 36-deficient mice. Neuron. 31:487–495.

Jinno S, Kosaka T. 2000. Colocalization of parvalbumin and somatostatin-like immunoreactivity in the mouse hippocampus: quantitative analysis with optical disector. J Comp Neurol. 428:377–388.

Jinno S, Kosaka T. 2002. Patterns of expression of calcium binding proteins and neuronal nitric oxide synthase in different populations of hippocampal GABAergic neurons in mice. J Comp Neurol. 449:1–25.

Kaneda M, Farrant M, Cull-Candy SG. 1995. Whole-cell and single-channel currents activated by GABA and glycine in granule cells of the rat cerebellum. J Physiol Lond. 485:419–435.

Kawaguchi Y, Kubota Y. 1997. GABAergic cell subtypes and their synaptic connections in rat frontal cortex. Cereb Cortex. 7:476–486.

Klausberger T, Magill PJ, Marton L, Roberts JDB, Cobden PM, Buzsáki G, Somogyi P. 2003. Brain state- and cell type-specific firing of hippocampal interneurons in vivo. Nature. 421:844–848.

Klausberger T, Marton LF, Baude A, Roberts JDB, Magill P, Somogyi P. 2004. Spike timing of dendrite-targeting bistratified cells during hippocampal network oscillations in vivo. Nat Neurosci. 7:41–47.

Klausberger T, Marton LF, O'Neill J, Huck JHJ, Dalezios Y, Fuentealba P, Suen WY, Papp E, Kaneko T, Watanabe M, et al. 2005. Complementary roles of cholecystokinin- and parvalbumin-expressing GABAergic neurons in hippocampal network oscillations. J Neurosci. 25: 9782–9793.

Klausberger T, Roberts JDB, Somogyi P. 2002. Cell type- and input-specific differences in the number and subtypes of synaptic GABA$_A$ receptors in the hippocampus. J Neurosci. 22:2513–2521.

Kosaka T, Katsumaru H, Hama K, Wu JY, Heizmann CW. 1987. GABAergic neurons containing the Ca2+-binding protein parvalbumin in the rat hippocampus and dentate gyrus. Brain Res. 419: 119–130.

LeBeau FE, Traub RD, Monyer H, Whittington MA, Buhl EH. 2003. The role of electrical signaling via gap junctions in the generation of fast network oscillations. Brain Res Bull. 62:3–13.

Losonczy A, Zhang L, Shigemoto R, Somogyi P, Nusser Z. 2002. Cell type dependence and variability in the short-term plasticity of EPSCs in identified mouse hippocampal interneurones. J Physiol. 542: 193–210.

Maccaferri G, Roberts JDB, Szucs P, Cottingham CA, Somogyi P. 2000. Cell surface domain specific postsynaptic currents evoked by identified GABAergic neurones in rat hippocampus in vitro. J Physiol Lond. 524:91–116.

Mann EO, Suckling JM, Hajos N, Greenfield SA, Paulsen O. 2005. Perisomatic feedback inhibition underlies cholinergically induced fast network oscillations in the rat hippocampus in vitro. Neuron. 45:105–117.

Markram H, Toledo-Rodriguez M, Wang Y, Gupta A, Silberberg G, Wu C. 2004. Interneurons of the neocortical inhibitory system. Nat Rev Neurosci. 5:793–807.

McKernan RM, Rosahl TW, Reynolds DS, Sur C, Wafford KA, Atack JR, Farrar S, Myers J, Cook G, Ferris P, et al. 2000. Sedative but not anxiolytic properties of benzodiazepines are mediated by the GABAA receptor α1 subtype. Nat Neurosci. 3:587–592.

Meyer AH, Katona I, Blatow M, Rozov A, Monyer H. 2002. In vivo labeling of parvalbumin-positive interneurons and analysis of electrical coupling in identified neurons. J Neurosci. 22:7055–7064.

Mithani S, Atmadja S, Baimbridge KG, Fibiger HC. 1987. Neuroleptic-induced oral dyskinesias: effects of progabide and lack of correlation with regional changes in glutamic acid decarboxylase and choline acetyltransferase activities. Psychopharmacology. 93:94–100.

Mohler H, Knoflach F, Paysan J, Motejlek K, Benke D, Luscher B, Fritschy JM. 1995. Heterogeneity of GABAA-receptors: cell-specific expression, pharmacology, and regulation. Neurochem Res. 20: 631–636.

Nusser Z, Mody I. 2002. Selective modulation of tonic and phasic inhibitions in dentate gyrus granule cells. J Neurophysiol. 87: 2624–2648.

Nusser Z, Roberts JDB, Baude A, Richards JG, Sieghart W, Somogyi P. 1995. Immunocytochemical localization of the α1 and β2/3 subunits of the GABAA receptor in relation to specific GABAergic synapses in the dentate gyrus. Eur J Neurosci. 7:630–646.

Nusser Z, Roberts JDB, Baude A, Richards JG, Somogyi P. 1995. Relative densities of synaptic and extrasynaptic GABAA receptors on cere-bellar granule cells as determined by a quantitative immunogold method. J Neurosci. 15:2948–2960.

Nusser Z, Sieghart W, Benke D, Fritschy J-M, Somogyi P. 1996. Differential synaptic localization of two major γ-aminobutyric acid type A receptor a subunits on hippocampal pyramidal cells. Proc Natl Acad Sci USA. 93:11939–11944.

Nyiri G, Freund TF, Somogyi P. 2001. Input-dependent synaptic targeting of α2-subunit-containing GABAA receptors in synapses of hippo-campal pyramidal cells of the rat. Eur J Neurosci. 13:428–442.

Oliva AA, Jiang M, Lam T, Smith KL, Swann JW. 2000. Novel hippocampal interneuronal subtypes identified using transgenic mice that express green fluorescent protein in GABAergic interneurons. J Neurosci. 20:3354–3368.

Pawelzik H, Bannister AP, Deuchars J, Ilia M, Thomson AM. 1999. Modulation of bistratified cell IPSPs and basket cell IPSPs by pentobarbitone sodium, diazepam and Zn2+: dual recordings in slices of adult rat hippocampus. Eur J Neurosci. 11:3552–3564.

Pawelzik H, Hughes DI, Thomson AM. 2002. Physiological and morpho-logical diversity of immunocytochemically defined parvalbumin- and cholecystokinin-positive interneurones in CA1 of the adult rat hippocampus. J Comp Neurol. 443:346–367.

Pinault D. 1996. A novel single-cell staining procedure performed in vivo under electrophysiological control: morpho-functional features of juxtacellularly labeled thalamic cells and other central neurons with biocytin or neurobiotin. J Neurosci Methods. 65:113–136.

Pirker S, Schwarzer C, Wieselthaler A, Sieghart W, Sperk G. 2000. GABA$_A$ receptors: immunocytochemical distribution of 13 subunits in the adult rat brain. Neuroscience. 101:815–850.

Pouille F, Scanziani M. 2001. Enforcement of temporal fidelity in pyramidal cells by somatic feed-forward inhibition. Science. 293: 1159–1163.

Price CJ, Cauli B, Kovacs ER, Kulik A, Lambolez B, Shigemoto R, Capogna M. 2005. Neurogliaform neurons form a novel inhibitory network in the hippocampal CA1 area. J Neurosci. 25:6775–6786.

Rudolph U, Crestani F, Benke D, Brunig I, Benson JA, Fritschy J-M, Martin JR, Bluethmann H, Mohler H. 1999. Benzodiazepine actions mediated by specific γ-aminobutyric acid$_A$ receptor subtypes. Nature. 401: 796–800.

Rudolph U, Mohler H. 2006. GABA-based therapeutic approaches: GABAA receptor subtype functions. Curr Opin Pharmacol. 6:18–23.

Semyanov A, Walker MC, Kullmann DM. 2003. GABA uptake regulates cortical excitability via cell type-specific tonic inhibition. Nat Neurosci. 6:484–490.

Semyanov A, Walker MC, Kullmann DM, Silver RA. 2004. Tonically active GABA$_A$ receptors: modulating gain and maintaining the tone. Trends Neurosci. 27:262–269.

Simon A, Olah S, Molnar G, Szabadics J, Tamas G. 2005. Gap-junctional coupling between neurogliaform cells and various interneuron types in the neocortex. J Neurosci. 25:6278–6285.

Sohl G, Odermatt B, Maxeiner S, Degen J, Willecke K. 2004. New insights into the expression and function of neural connexins with transgenic mouse mutants. Brain Res Brain Res Rev. 47:245-259.

Somogyi J, Baude A, Omori Y, Shimizu H, El Mestikawy S, Fukaya M, Shigemoto R, Watanabe M, Somogyi P. 2004. GABAergic basket cells expressing cholecystokinin contain vesicular glutamate transporter type 3 (VGLUT3) in their synaptic terminals in hippocampus and isocortex of the rat. Eur J Neurosci. 19:552-569.

Somogyi P, Fritschy J-M, Benke D, Roberts JDB, Sieghart W. 1996. The γ2 subunit of the GABAA receptor is concentrated in synaptic junctions containing the α1 and β2/3 subunits in hippocampus, cerebellum and globus pallidus. Neuropharmacology. 35:1425-1444.

Somogyi P, Klausberger T. 2005. Defined types of cortical interneurone structure space and spike timing in the hippocampus. J Physiol. 562:9-26.

Sugino K, Hempel CM, Miller MN, Hattox AM, Shapiro P, Wu C, Huang ZJ, Nelson SB. 2006. Molecular taxonomy of major neuronal classes in the adult mouse forebrain. Nat Neurosci. 9:99-107.

Sur C, Wafford KA, Reynolds DS, Hadingham KL, Bromidge F, Macaulay A, Collinson N, O'Meara G, Howell O, Newman R, et al. 2001. Loss of the major GABA$_A$ receptor subtype in the brain is not lethal in mice. J Neurosci. 21:3409-3418.

Szabadics J, Lorincz A, Tamas G. 2001. β and γ frequency synchronization by dendritic GABAergic synapses and gap junctions in a network of cortical interneurons. J Neurosci. 21:5824-5831.

Szabadics J, Varga C, Molnar G, Olah S, Barzo P, Tamas G. 2006. Excitatory effect of GABAergic axo-axonic cells in cortical microcircuits. Science. 311:233-235.

Tamas G, Buhl EH, Lorincz A, Somogyi P. 2000. Proximally targeted GABAergic synapses and gap junctions synchronize cortical interneurons. Nat Neurosci. 3:366-371.

Tretter V, Ehya N, Fuchs K, Sieghart W. 1997. Stoichiometry and assembly of a recombinant GABAA receptor subtype. J Neurosci. 17:2728-2737.

Venance L, Rozov A, Blatow M, Burnashev N, Feldmeyer D, Monyer H. 2000. Connexin expression in electrically coupled postnatal rat brain neurons. Proc Natl Acad Sci USA. 97:10260-10265.

Vida I, Bartos M, Jonas P. 2006. Shunting inhibition improves robustness of gamma oscillations in hippocampal interneuron networks by homogenizing firing rates. Neuron. 49:107-117.

Vincent SR, McIntosh CH, Buchan AM, Brown JC. 1985. Central somatostatin systems revealed with monoclonal antibodies. J Comp Neurol. 238:169-186.

Vogt A, Hormuzdi SG, Monyer H. 2005. Pannexin1 and Pannexin2 expression in the developing and mature rat brain. Mol Brain Res. 141:113-120.

Weickert S, Ray A, Georg Z, Dermietzel R. 2005. Expression of neural connexins and pannexin1 in the hippocampus and inferior olive: a quantitative approach. Mol Brain Res. 133:102-109.

Whittington MA, Traub RD. 2003. Interneuron diversity series: inhibitory interneurons and network oscillations in vitro. Trends Neurosci. 26:676-682.

Wisden W, Laurie DJ, Monyer H, Seeburg PH. 1992. The distribution of 13 GABAA receptor subunit mRNAs in the rat brain. I. Telencephalon, diencephalon, mesencephalon. J Neurosci. 12:1040-1062.

Zezula J, Fuchs K, Sieghart W. 1991. Separation of alpha 1, alpha 2 and alpha 3 subunits of the GABAA-benzodiazepine receptor complex by immunoaffinity chromatography. Brain Res. 563:325-328.

Zsiros V, Maccaferri G. 2005. Electrical coupling between interneurons with different excitable properties in the stratum lacunosum-moleculare of the juvenile CA1 rat hippocampus. J Neurosci. 25:8686-8695.